Quasi one-dimensional Bose–Einstein condensate in a gravito-optical surface trap

2016 J. Phys. B: At. Mol. Opt. Phys. 49 075302

(http://iopscience.iop.org/0953-4075/49/7/075302)

IOP Publishing Journal of Physics B: Atomic, Molecular and Optical Physics
J. Phys. B: At. Mol. Opt. Phys. **49** (2016) 075302 (10pp) doi:10.1088/0953-4075/49/7/075302

Quasi one-dimensional Bose–Einstein condensate in a gravito-optical surface trap

Javed Akram[1,2,6], **Benjamin Girodias**[3,4] **and Axel Pelster**[5]

[1] Institute für Theoretische Physik, Freie Universität Berlin, Arnimallee 14, D-14195 Berlin, Germany
[2] Department of Physics, COMSATS, Institute of Information Technology Islamabad, Pakistan
[3] Department of Physics and Astronomy, Pomona College, CA, USA
[4] Department of Physics, University of Michigan, MI, USA
[5] Fachbereich Physik und Forschungszentrum OPTIMAS, Technische Universität Kaiserslautern, Germany

E-mail: javedakram@daad-alumni.de, bgiro@umich.edu and axel.pelster@physik.uni-kl.de

Received 14 November 2015, revised 30 January 2016
Accepted for publication 10 February 2016
Published 17 March 2016

Abstract

We study both static and dynamic properties of a weakly interacting Bose–Einstein condensate (BEC) in a quasi one-dimensional gravito-optical surface trap, where the downward pull of gravity is compensated by the exponentially decaying potential of an evanescent wave. First, we work out approximate solutions of the Gross–Pitaevskii equation for both a small number of atoms using a Gaussian ansatz and a larger number of atoms using the Thomas–Fermi limit. Then we confirm the accuracy of these analytical solutions by comparing them to numerical results. From there, we numerically analyze how the BEC cloud expands non-ballistically, when the confining evanescent laser beam is shut off, showing agreement between our theoretical and previous experimental results. Furthermore, we analyze how the BEC cloud expands non-ballistically due to gravity after switching off the evanescent laser field in the presence of a hard-wall mirror which we model by using a blue-detuned far-off-resonant sheet of light. There we find that the BEC shows significant self-interference patterns for a large number of atoms, whereas for a small number of atoms, a revival of the BEC wave packet with few matter-wave interference patterns is observed.

Keywords: Bose–Einstein condensate, matter-wave interference, guasi one-dimensional, gravito-optical, surface trap

(Some figures may appear in colour only in the online journal)

1. Introduction

Bose–Einstein condensation (BEC) is impossible in a one- or a two-dimensional homogeneous system [1, 2], but does occur in atomic traps because the confining potential modifies the density of states [3–5]. Experimentally, a highly elongated quasi-1D regime can be reached by tightly confining the atoms in the radial direction, which can be effectively achieved by letting the radial frequency be much larger than the axial frequency [6–13]. However, when the radial length scales become as the order of the atomic interaction length, the one-dimensional system can only be described within the Tonks–Girardeau or within the super-Tonks–Girardeau regime [14–16], which is experimentally reachable near a confinement-induced resonance [17–19].

The interaction of lower dimensional ultra-cold atoms with surfaces has attracted much attention in the past few years as their enhanced quantum and thermal fluctuations have turned out to play an important role for various technological applications [20–23]. Also under such circumstances, the influence of gravity must be taken into account. For many years, atomic mirrors were constructed in the presence of a gravitational field by using repulsive evanescent waves, which reflect both atomic beams and cold atom clouds [24–26]. The trapping of atoms in a gravitational cavity, consisting of a single horizontal concave mirror placed in a gravitational field, is discussed in detail in [27, 28]. The inherent losses of atoms in a gravitational cavity can be reduced by using a higher detuning between the evanescent wave and the atomic resonance frequency in a gravitational trap [29]. In 1996, Marzlin and Audretsch

[6] Author to whom all correspondence should be addressed.

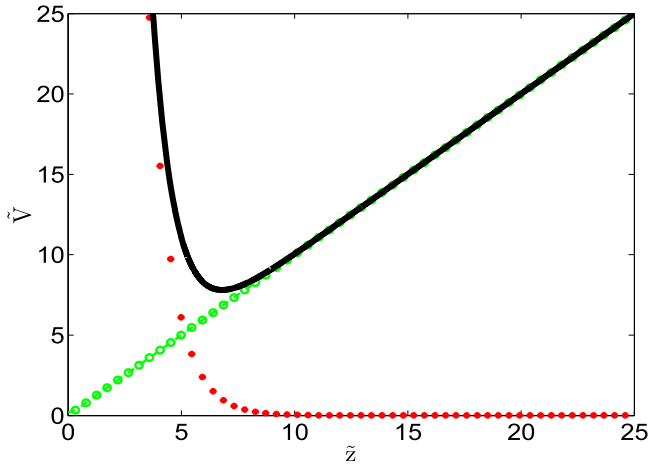

Figure 1. Anharmonic GOST potential (solid line) from equation (2) in dimensionless units, which are explained at the end of the section 2. It consists of a superposition of an exponentially decaying optical potential (red circles) due to an evanescent light field above a mirror and a linear gravitational potential (dashed-green circles). When the atoms are cold enough, they stay in the vicinity of the potential minimum.

studied the trapping of three-level atoms in a gravito-optical trap by using the trampolining technique without the trampoline [30]. Another approach proposed by Saif *et al*, uses a spatially periodic modulated atomic mirror to yield either a localization [31] or a coherent acceleration [32] of material wave packets depending on the chosen initial conditions and the respective system parameters. In 2002, Nesvizhevsky *et al* reported the evidence of gravitational quantum bound states of neutrons in a gravitational cavity [33]. Not only is a good confinement geometry necessary for trapping and observing the dynamics of atoms, but an experiment also needs an efficient loading scheme loading scheme. The experimental group of Rudi Grimm from Innsbruck demonstrated both the loading of ^{133}Cs atoms [34, 35] and the subsequent creation of a BEC in a quasi-2D gravito-optical surface trap (GOST) [36, 37]. More recently, Colombe *et al* studied the scheme for loading a ^{87}Rb BEC into a quasi-2D evanescent light trap and observed the diffraction of a BEC in the time domain [38, 39]. Later Perrin et at. studied the diffuse reflection of a BEC from a rough evanescent wave mirror [40].

Motivated by the crucial relevance of gravito-optical surface traps in atomic waveguides [41–43] and atomic chips [44–47], in this paper we study the special case of a quasi one-dimensional Bose–Einstein condensate which is trapped orthogonal to the prism surface along the vertical axis. In our proposed model the downward pull of gravity is compensated by an exponentially decaying evanescent wave (EW), which can be thought of as a mirror as it repels the atoms upward against gravity as shown in figure 1. In order to deal with the hard-wall boundary condition, we apply the mirror solution analogy to the BEC context, and obtain analytical results, which agree with those from numerically solving the underlying one-dimensional Gross–Pitaevskii equation (1DGPE). Later on, as an interesting application, we compare our numerical simulation results for a time-of-flight dynamics with the Innsbruck experiment for a quasi-2D BEC in a GOST [37]. Surprisingly, our proposed quasi one-dimensional model agrees even quantitatively with the Innsbruck experiment. Although this Innsbruck experiment uses a 2D pancake-shaped BEC, when performing the time-of-flight expansion vertically the transversely confining beam is kept constant, so our quasi-1D model for a BEC should apply in this case.

The paper is organized as follows, the underlying fundamental model for such a quasi-1D BEC is reviewed in section 2. Furthermore, we provide estimates for experimentally realistic parameters, which we use in our quantitative analysis. Afterwards, we work out approximate solutions for the 1DGPE wave function in the ground state of the system. To this end, section 3 performs a modified Gaussian variational ansatz for weak interactions, which corresponds to a small number of atoms. For a larger number of atoms, the interaction strength becomes so strong that the Thomas–Fermi solution turns out to be valid, as described in section 4. Then, in section 5, we outline our numerical methods and compare them to the previous analytical solutions. In section 6, we deal with the time-of-flight expansion of the BEC when the EW is removed, showing quantitative agreement with previous experimental results. In section 7 we discuss further dynamical properties of the BEC in a GOST after switching off the evanescent laser field in the presence of the hard-wall mirror. Lastly, we summarize our findings and end with brief concluding remarks.

2. Model

For our 1D model of the BEC in a GOST, we assume that we have a dilute Bose gas and that the radial frequency is much larger than the axial frequency, i.e. the BEC is cigar-shaped. With this assumption, we arrive at the 1DGPE [48, 49]

$$\mathrm{i}\hbar\frac{\partial}{\partial t}\psi(z,t)=\left\{-\frac{\hbar^2}{2m_\mathrm{B}}\frac{\partial^2}{\partial z^2}+V(z)\right.$$
$$\left.+\,\mathrm{G_B}\,|\psi(z,t)|^2\right\}\psi(z,t). \qquad (1)$$

On the right-hand side of the equation, the first term represents the kinetic energy of the atoms with mass m_B, while the last term describes the two-particle interaction, where its strength $\mathrm{G_B}=2N_\mathrm{B}a_\mathrm{B}\hbar\omega_r$ is related to the s-wave scattering length a_B, and the particle number N_B, whereas ω_r denotes the radial trapping frequency. The anharmonic potential energy $V(z)$ in equation (1) is produced by both gravity and the exponentially decaying evanescent wave as shown in figure 1 [2]:

$$V(z)=V_0\mathrm{e}^{-\kappa z}+m_\mathrm{B}\mathrm{g}z. \qquad (2)$$

Here, g is the gravitational acceleration and the constant $V_0 = \Gamma\lambda_0^3 I_0/(8\pi^2 c\delta_3)$ denotes the strength of the evanescent field, where Γ is the natural linewidth of ^{133}Cs atoms, $\lambda_0 = 852$ nm is the wavelength of the optical transition, I_0 stands for the peak intensity of the EW, and δ_3 corresponds to the detuning frequency of the hyperfine sub-level $F = 3$ of the ^{133}Cs atom [34, 35, 37]. Furthermore, $1/\kappa = \Lambda/2 = \lambda/4\pi\sqrt{n^2\sin^2\theta - 1}$ represents the decay length, where λ is the wavelength of the EW, n stands for the refractive index of the medium and θ is the angle of incidence. The potential equation (2) has a minimum at $z_0^{\min} = (1/\kappa)\ln(V_0\kappa/m_B g)$ with the axial frequency $\omega_z = \sqrt{g\kappa}$. Note that this potential yields a hard-wall condition with $V(z \leqslant 0) = \infty$, because the atoms cannot penetrate the prism, as it is a macroscopic object.

In order to have a concrete set-up in mind for our analysis, we adapt parameter values from the GOST experiments [34, 37]. For the EW, we consider the inverse decay length to be $\kappa = 2/\Lambda = 1.43 \times 10^6$ m^{-1}, i.e. $\Lambda \approx 1.4$ μm. Additionally, we assume an axial frequency of $\omega_z \approx 2\pi \times 600$ Hz. For our atoms in the $F = 3$ state, the strength of the EW is given by $V_0 \approx 100 \times k_B$ μK, where k_B is the Boltzmann constant. This potential value is within an order of magnitude of the Innsbruck experiments [34, 37]. In view of the quasi-1D model, we must satisfy the condition $\omega_z \ll \omega_r$, so we assume $\omega_r = 2\pi \times 3$ kHz, which corresponds to the radial oscillator length $l_r = 0.892$ μm. The experiment uses a magnetic field for Feshbach resonance, such that the s-wave scattering length amounts to $a_B = 440$ a_0 with the Bohr radius a_0. As both $\omega_z \ll \omega_r$ and $l_r > a_B$ are fulfilled, we have, indeed, a quasi one-dimensional setting.

When the atoms are close to the dielectric surface of the prism, we would have to add an additional potential contribution due to the van-der-Waals interaction. Here we have to distinguish two special cases depending on the distance of the BEC from the surface. The regime, where the BEC is close to the dielectric surface, i.e. $z \ll \lambda/2\pi$, is called the Lennard–Jones regime [50, 51]. In the case where the BEC is far away from the surface, i.e. $z \gg \lambda/2\pi$, the regime is called Casimir–Polder regime. In the latter case the Casimir–Polder potential can be described within a two-level approximation of the Cesium atoms according to $V_{CP} = -C_4/z^4$, where the Casimir–Polder coefficient is $C_4 = 1.78 \times 10^{-55}$Jm^4 [52–54]. As the BEC does not penetrate very far into the repulsive EW, it is hardly influenced by the van-der-Waals potential, which follows from the above values of the GOST experiment. Indeed, for the wavelength $\lambda = 839$ nm [37] and the distance being estimated by the minimal distance of the BEC from the surface $z_0^{\min} = 4.761$ μm, we are in the the Casimir–Polder regime. Thus, the value of the Casimir–Polder potential is of the order $V_{CP} = 24.9 \times k_B$ pK, which is negligible in comparison with the EW potential $V_0 \approx 100 \times k_B$ μK.

In view of the forthcoming discussion we use dimensionless parameters as follows. First we introduce the dimensionless spatial coordinate $\tilde{z} = \kappa z$. Further, we multiply all terms in equation (1) by $\kappa/(m_B g)$, yielding the dimensionless GPE,

$$i\frac{\partial}{\partial\tilde{t}}\tilde{\psi}(\tilde{z},\tilde{t}) = \left\{-\frac{k}{2}\frac{\partial^2}{\partial\tilde{z}^2} + \tilde{z} + \tilde{V}_0 e^{-\tilde{z}} + \tilde{G}_B|\tilde{\psi}(\tilde{z},\tilde{t})|^2\right\}\tilde{\psi}(\tilde{z},\tilde{t}), \quad (3)$$

where the dimensionless kinetic energy constant reads $k = (\hbar^2\kappa^3)/(g m_B^2)$, the dimensionless time $\tilde{t} = t(m_B g)/(\hbar\kappa)$ and the two-particle dimensionless interaction strength $\tilde{G}_B = 2N_B\tilde{\omega}_r\tilde{a}_B$ with $\tilde{a}_B = a_B\kappa$ being a dimensionless s-wave scattering length. Additionally, we measure energies in units of the gravitational energy $m_B g/\kappa$ and get $\tilde{\omega}_z = \hbar\kappa\omega_z/g m_B$ as a dimensionless frequency, and $\tilde{V}_0 = \kappa V_0/g m_B$ as a dimensionless strength of the evanescent field.

According to these chosen parameters, the dimensionless quantities have the following values. The dimensionless strength of the EW is $\tilde{V}_0 = 905.7$, the dimensionless kinetic energy amounts to $\tilde{k} = 0.066$, the dimensionless s-wave scattering length is given by $\tilde{a}_B = 0.033$, the dimensionless radial frequency yields $\tilde{\omega}_r = 1.303$, and, finally, the resulting dimensionless two-particle interaction strength is $\tilde{G}_B = 0.086N_B$. From here on, we will drop the tildes for simplicity.

3. Variational solution

For the number of particles $N_B < 3000$, the effective interaction strength is quite small. In this limit the BEC has only a reduced extension, so the anharmonic confinement $V(z)$ approximately corresponds to a harmonic potential well around its minimum $z_0^{\min} \approx 6.809$. Therefore, it is reasonable to propose a Gaussian-like ansatz for the wave function in the static case. In order to meet the hard-wall condition, however, we modify the Gaussian function such that it has the form of a so-called mirror solution [55, 56],

$$\psi(z) \propto \exp\left[\frac{-(z - z_0)^2}{2A^2}\right] - \exp\left[\frac{-(z + z_0)^2}{2A^2}\right], \quad (4)$$

where z_0 is the mean position and A represents the width. In this way it is guaranteed that the wave function meets the hard-wall boundary condition $\psi(0) = 0$. In order to find the variational parameters z_0 and A, we minimize the energy of this ansatz following the idea of Perez *et al* [57, 58]. In order to simplify the expression for the corresponding energy, we introduce the parameter $\gamma = z_0/A$ and normalize the wave function (4) to obtain

$$\psi(z) = \frac{\exp\left(-\frac{z^2}{2A^2}\right)\mathrm{Sinh}\left(\frac{\gamma z}{A}\right)}{\sqrt{\frac{A}{4}\sqrt{\pi}\left[\exp(\gamma^2) - 1\right]}}. \quad (5)$$

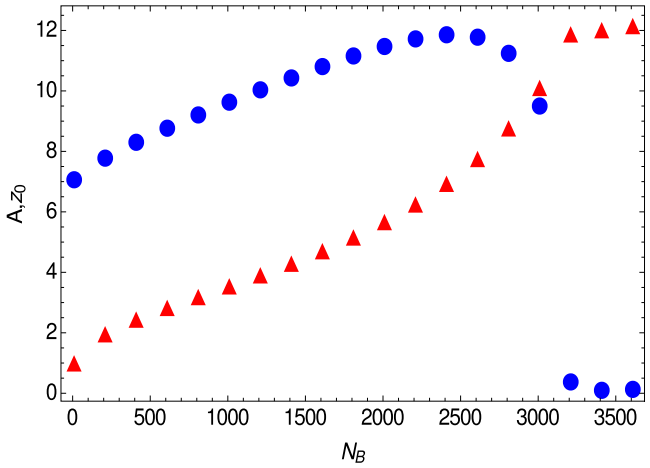

Figure 2. Width A (triangles) and mean position z_0 (circles) as a function of the number of atoms N_B. Note that the mean position gives meaningless values for $N_B > 3000$. Thus, the variational ansatz is only successful for quite a small number of particles.

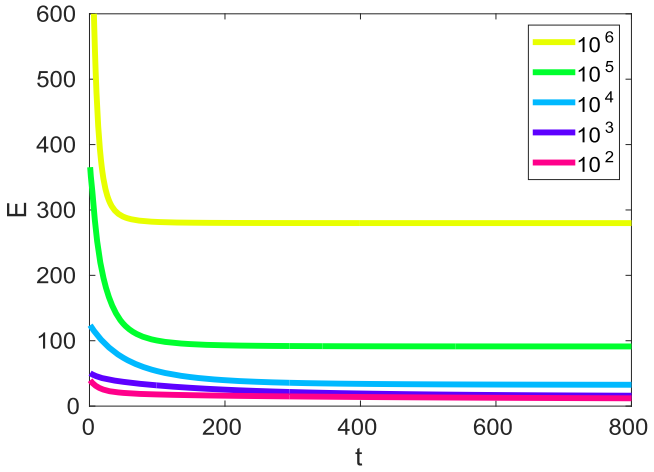

Figure 3. Energy of the BEC as a function of imaginary time for a decreasing number of particles from the top to the bottom.

From this ansatz, we obtain the Gross–Pitaevskii energy

$$E = \frac{V_0\left\{e^{\frac{1}{4}(A-2\gamma)^2}\left[\mathrm{Erfc}\left(\frac{A}{2}-\gamma\right)+e^{2A\gamma}\mathrm{Erfc}\left(\frac{A}{2}+\gamma\right)\right]-2e^{\frac{A^2}{4}}\mathrm{Erfc}\left(\frac{A}{2}\right)\right\}}{2(e^{\gamma^2}-1)} + \frac{2Ae^{\gamma^2}\gamma\,\mathrm{Erf}(\gamma)}{2(e^{\gamma^2}-1)} + \frac{(2\gamma^2+e^{\gamma^2}-1)k}{4A^2(e^{\gamma^2}-1)} + \frac{\left[2\left(e^{\frac{\gamma^2}{2}}+1\right)^{-2}+1\right]G_B}{2\sqrt{2\pi}A}. \quad (6)$$

where $\mathrm{Erf}(y) = \frac{2}{\sqrt{\pi}}\int_0^y e^{-x^2}dx = 1 - \mathrm{Erfc}(y)$ denotes the error function. Although, this expression cannot be minimized analytically, we can use numerical techniques to extremize it with respect to the parameters γ and A based on the values of k, G_B, and V_0 given in section 2. We can see from figure 2 that our variational approach turns out to be valid only for quite a small number of atoms. Indeed, the extremization process fails when the condensate has more than around 3000 atoms, as then the mean position becomes zero as shown in figure 2. Note that BEC experiments with such small particle numbers are possible, see for instance [59, 60].

4. Thomas–Fermi limit solution

For a large enough number of atoms, the effective interaction term and the potential term are much larger than the kinetic term. In such a case, an approximate Thomas–Fermi (TF) solution is found by neglecting the much smaller kinetic term. Thus, the time-independent GPE reduces to

$$\mu \approx z + V_0 e^{-z} + G_B\,|\psi(z)|^2. \quad (7)$$

In order to determine the chemical potential, we use the normalization condition, which reads in the dimensionless scheme as $\int|\psi|^2dz = 1$. Thus, we get

$$1 = \frac{\mu}{G_B}\int_{z_1}^{z_2}\left(1 - \frac{z}{\mu} - \frac{V_0}{\mu}e^{-z}\right)dz, \quad (8)$$

where z_1 and z_2 denote the zeros of the integrand. For larger z the decaying exponential vanishes, and so we have $z_2 \approx \mu$. Examining the smaller root, we see that for small values of z and moderate values of μ, z/μ is quite small, thus a reasonable approximation for this root is $z_1 \approx \log(V_0/\mu)$. This motivates us to divide the TF solution into two parts: first, the soft-wall TF solution, where $V_0 > \mu$, so that z_1 is larger than zero. Second, the hard-wall TF solution in the case $V_0 < \mu$, where the lower integration limit z_1 would be less than zero, so the soft-wall TF wave function would fail. The latter case necessitates to use the mirror principle in order to guarantee the hard-wall boundary condition.

4.1. Soft-wall TF solution

With the integration boundaries $z_1 \approx \log(V_0/\mu)$ and $z_2 \approx \mu$ known to be a good approximation, we carry out the integration in equation (8), yielding

$$2G_B \approx \mu^2\left\{1 - \frac{2}{\mu}\left[\log\left(\frac{V_0}{\mu}\right)+1\right]\right\}, \quad (9)$$

where we have neglected the small terms $(V_0/\mu)e^{-\mu}$ and $\log(V_0/\mu)^2/(2\mu)$. Thus, to leading order, we have $\mu \approx \sqrt{2G_B}$ with a subsequent logarithmic correction. For small changes of the chemical potential, the natural log term

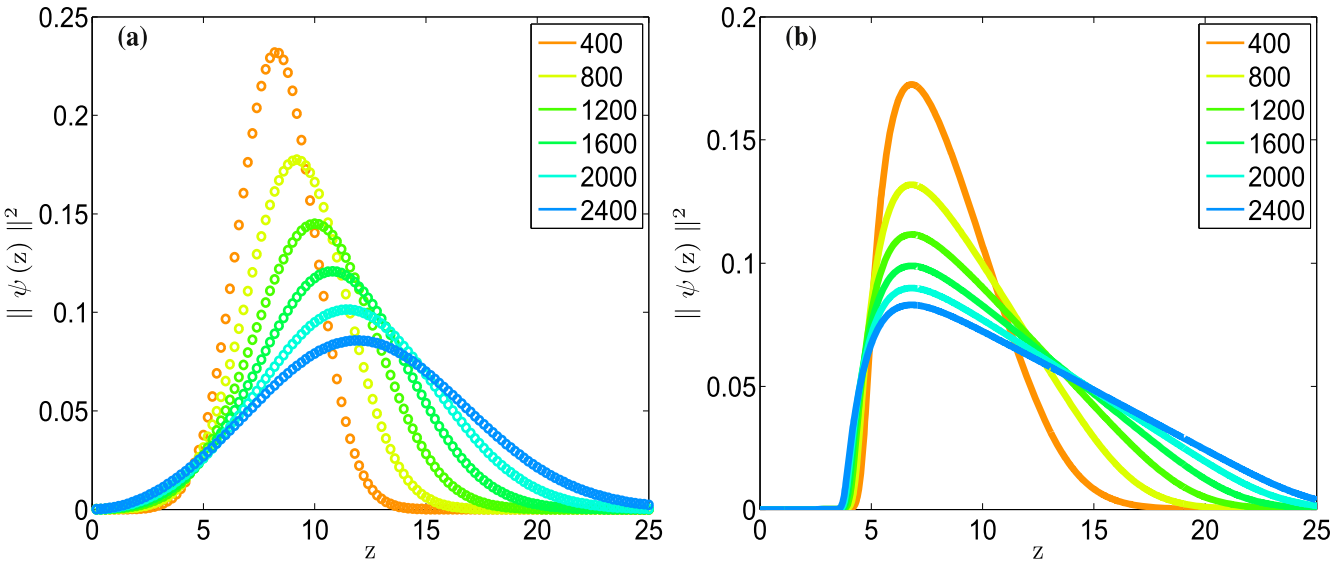

Figure 4. Probability density plots from (a) Gaussian ansatz (5) and (b) numerical calculations for an increasing number of atoms from the top to the bottom.

in equation (9) does not change significantly. Therefore in equation (9) we can substitute $\sqrt{2G_B}$ for μ in the natural log. Using the quadratic equation and neglecting small terms in the square root, we obtain the improved approximation

$$\mu \approx \sqrt{2G_B} + 1 + \log(V_0/\sqrt{2G_B}). \tag{10}$$

Thus, assuming that $V_0 > \sqrt{2G_B}$, we obtain the following soft-wall TF solution for $z_1 < z < z_2$.

$$\psi(z) = \sqrt{\frac{\mu}{G_B}\left(1 - \frac{z}{\mu} - \frac{V_0}{\mu}e^{-z}\right)}, \tag{11}$$

where μ is given by equation (10). The function is set to zero for $z < z_1 \approx \log(V_0/\sqrt{2G})$ and $z > z_2 \approx \mu$, because the probability density cannot be less than zero.

4.2. Hard-wall TF solution

For particle numbers $N_B > 2.35 \times 10^5$ the soft-wall TF solution is not valid anymore as $z_1 \approx \log(V_0/\sqrt{2G_B})$ becomes negative. In order to extend this approximate solution to the case where $V_0 < \mu$, we must work out the corresponding hard-wall TF solution. With the help of the mirror analogy [55, 56], we obtain the approximate TF wave function

$$\psi(z) = \begin{cases} \sqrt{\frac{1}{M}}\left[\sqrt{\left(\frac{\mu}{G_B}\right)\left(1 - \frac{z}{\mu} - \frac{V_0}{\mu}e^{-z}\right)}\right. \\ \left. -\sqrt{\left(\frac{\mu}{G_B}\right)\left(1 + \frac{z}{\mu} - \frac{V_0}{\mu}e^{+z}\right)}\right] & \text{for } 0 < z < |z_1| \\ \sqrt{\frac{1}{M}\left(\frac{\mu}{G_B}\right)\left(1 - \frac{z}{\mu} - \frac{V_0}{\mu}e^{-z}\right)} & \text{for } |z_1| < z < z_2. \end{cases} \tag{12}$$

Here, M denotes the normalization constant which is determined from $\int|\psi|^2 dz = 1$. Note that an analytical derivation of M is not possible, therefore, we performed the respective integration numerically.

5. Numerical methods and results

In order to demonstrate the validity of the proposed analytical results, we numerically find the ground state of the wave function by propagating the GPE in imaginary time, with the help of the split operator technique [61–65]. For the above mentioned experimental parameters and with the value of N_B ranging from 10^6 to 10^6 atoms, the ground-state energy of the BEC in a GOST does, indeed, quickly converge as shown in figure 3.

With this technique in mind, we compare our analytical results from sections 3 and 4 to numerical results and show how the BEC wave function in a GOST changes with increasing the number of atoms. For a smaller number of atoms, the variational Gaussian ansatz is more suitable as shown in figure 4, whereas for a larger number of atoms the TF approximation turns out to be quite accurate as shown in figure 5. The variational Gaussian ansatz roughly reproduces the mean, but it is rather symmetrical, unlike the numerical results as the number of atoms approach 2400, see figure 4. Qualitatively, the BEC width is proportional to the number of atoms in a GOST. However, due to the EW decaying exponential potential, the BEC cannot expand in the negative z-

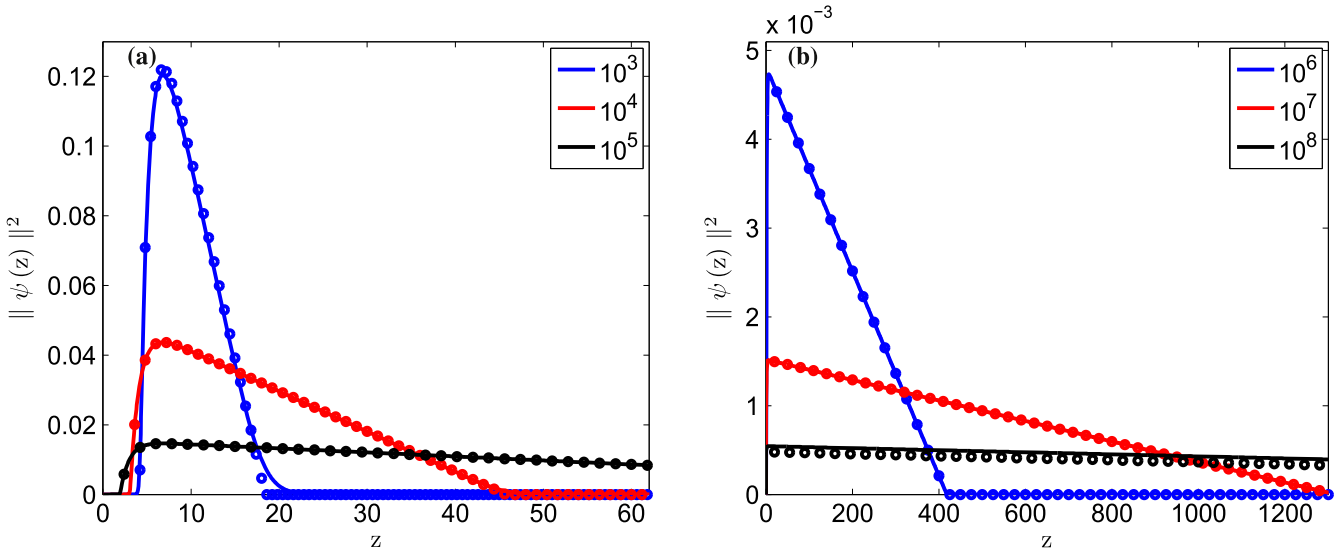

Figure 5. Comparison of numerical results from GPE (solid lines) with TF approximation (circles), (a) $N_B = 10^3$, $N_B = 10^4$, and $N_B = 10^5$. (b) $N_B = 10^6$, $N_B = 10^7$, and $N_B = 10^8$ from top to bottom, respectively.

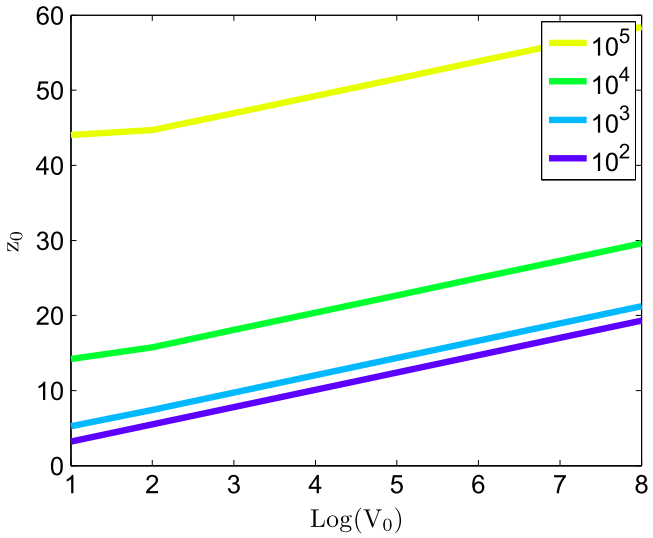

Figure 6. Mean position of the BEC versus EW strength V_0 for decreasing number of atoms from the top to the bottom.

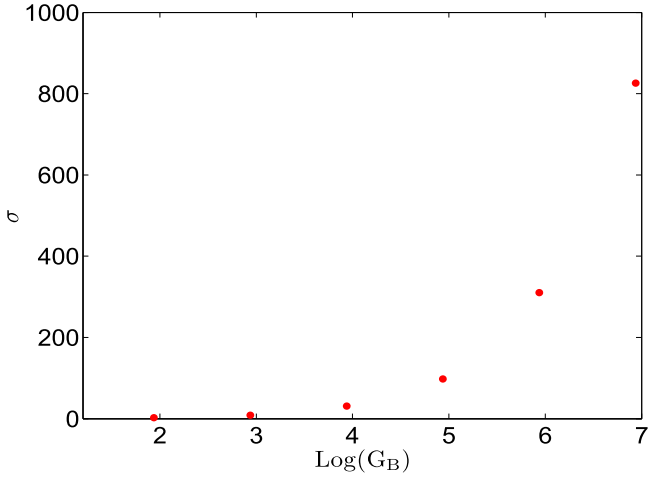

Figure 7. Standard deviation σ of BEC wave function increases with inter-particle interaction strength G_B for EW strength $V_0 = 906$.

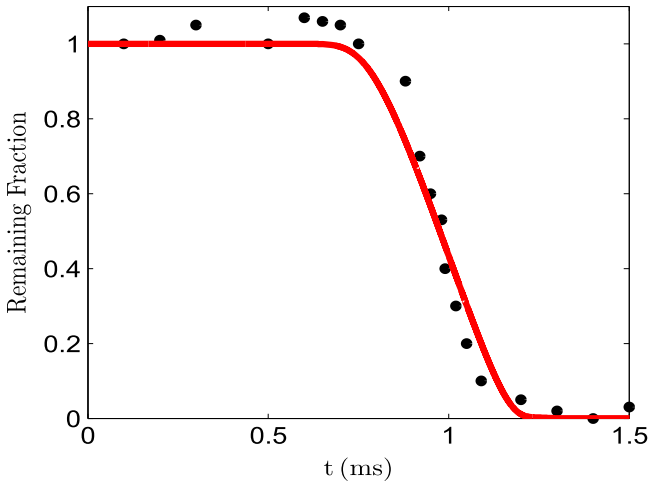

Figure 8. Fraction of remaining atoms during time-of-flight during a vertical expansion for $V_0 = 453$. Initially, total number of atoms is $N_B = 2400$. Here the circles stem from the Innsbruck experiment, whereas the solid line shows our numerical results. Figure reproduced from [37] with permission.

direction, so the BEC wave function takes up a triangular shape for N_B larger than 10^6 as shown in figure 5. The agreement between numerical and analytical TF results is much better for larger number of atoms. Note that the BEC wave function is quite wide for 10^8 atoms in figure 5.

The van der Waal forces with the surface can demolish the BEC, so it is necessary to have a larger EW potential. Therefore, keeping in mind recent developments in the laser field technology, it is possible to increase the EW strength V_0 by increasing the laser power [66]. Thus, we explore now the parameter space of our model. Irrespective of the number of atoms, the mean position of the BEC in GOST increases only moderately with V_0. For the soft-wall case $V_0 > \mu$ as shown in figure 6, the maximum of the wave function occurs at $\log(V_0)$, but for the hard-wall case $V_0 < \mu$ the maximum of the BEC

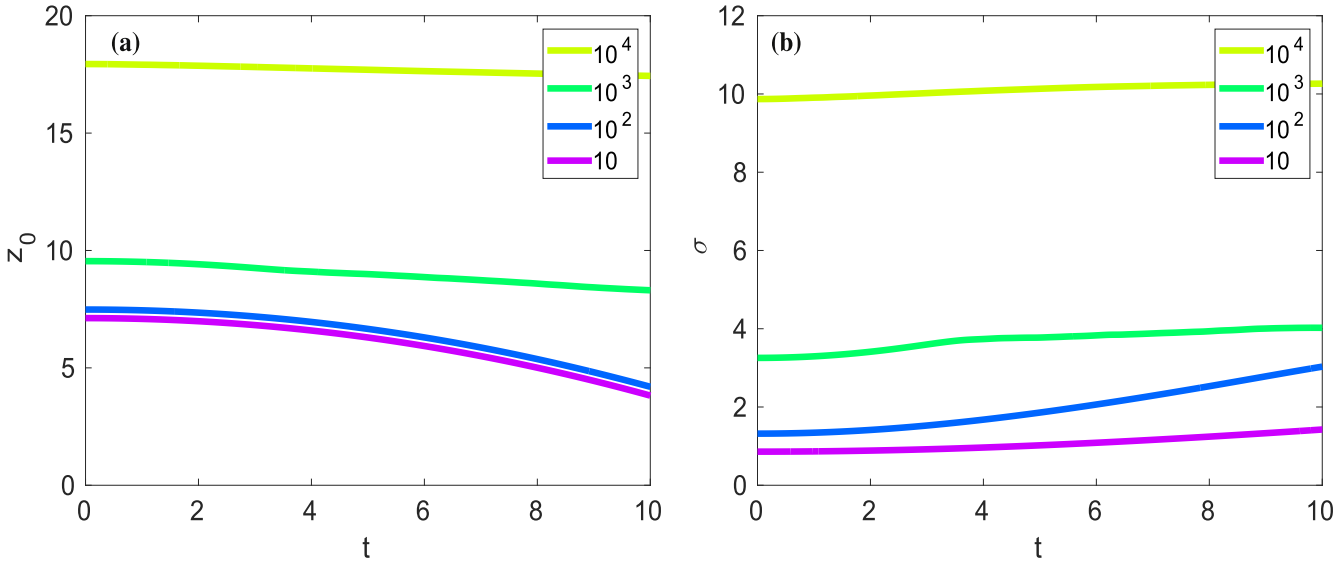

Figure 9. (a) Mean position z_0 and (b) standard deviation σ of BEC density in the time-of-flight expansion for decreasing number of atoms from the top to the bottom for $V_0 = 906$.

wave function exists at $|\log(V_0/\sqrt{2G_B})|$. Thus, due to the interaction term, for a large number of atoms, the maximum of the wave function no longer remains within the minimum of the trapping potential $z_0^{\min} \approx \log(V_0)$.

The BEC wave function in a GOST becomes asymmetric for larger interaction strengths. Therefore we quantify the BEC width based on the standard deviation $\sigma = \sqrt{\langle z^2\rangle - \langle z\rangle^2}$, where $\langle \bullet \rangle = \int \bullet |\psi(z)|^2 \mathrm{d}z$ denotes the expectation value. As shown in figure 7, the BEC standard deviation grows extremely rapidly with increasing number of atoms N_B. However, on the other hand, changing V_0 only slightly affects the standard deviation σ.

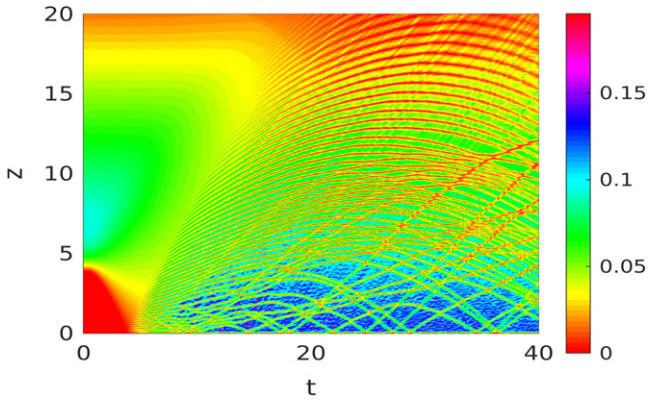

Figure 10. Dynamics of BEC in presence of gravity with hard wall at $z = 0$ for $N_B = 1800$ number of atoms. Here the color scale represents the density of the BEC.

6. Time-of-flight (TOF) expansion

The standard observation of a BEC is based on suddenly turning off the trapping potential and allowing the atoms to expand non-ballistically. The resulting time-of-flight (TOF) measurements are performed either by acquiring the absorption signal of the probe laser beam through the falling and expanding BEC cloud, or by measuring the fluorescence of the atoms which are excited by a resonant probe light [40].

In the Innsbruck experiment, the remaining number of atoms is measured after allowing atoms from the GOST to expand vertically by suddenly turning off the EW [37]. Note that some particles are lost due to thermalization processes which occur when the particles hit the prism or due to the van der Waal forces with the surface. Although this Innsbruck experiment uses a 2D pancake-shaped BEC, when performing this vertical expansion the transversally confining beam is kept constant, so our quasi-1D model for BEC should apply in this case. Using the experimental parameters in [37], we numerically reproduce their vertical expansion curve (their figure 2), as shown in figure 8. To this end, we use $N_B = 2400$ atoms and $V_0 = 453$, yielding an initial condensate wave function with dimensionless standard deviation $\sigma = 0.86$ and the dimensionless mean position $z_0 = 6.40$. We propagate this wave function without the hard-wall boundary condition. Then we approximate the fraction of remaining atoms by $\int_0^\infty |\psi(z, t)|^2 \mathrm{d}z$, as atoms in the BEC wave function extending past $z = 0$ are lost by sticking to the surface. As the interaction term is quite small in the Innsbruck experiment, the standard deviation of the BEC is small and remains roughly constant during the TOF, so the loss of atoms does not affect TOF expansion significantly for $t < 0.7$ ms as shown in figure 8.

We also simulated the TOF expansion without the prism at $z = 0$ for different particle numbers N_B. We see that the mean position of the BEC drops due to gravity as shown in figure 9 with different rates, which strongly depend upon the number of confined atoms. At the same time the BEC width, which is proportional to the standard deviation, increases according to figure 9.

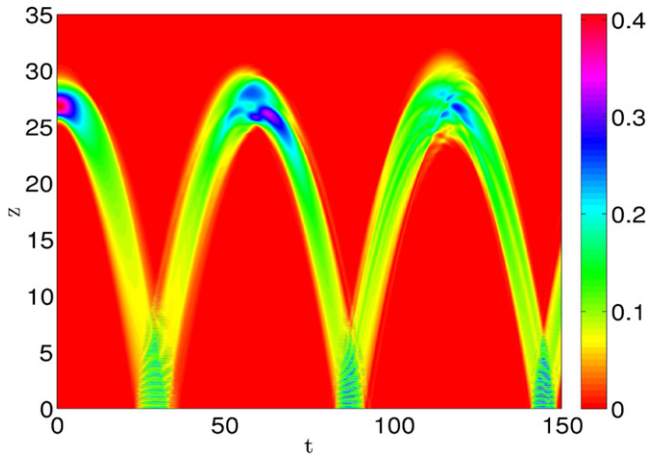

Figure 11. Numerical results for the BEC density $|\psi(z, t)|^2$ with initial dimensionless mean position $z_0 = 27.2$ and dimensionless standard deviation $\sigma = 0.99$ for $N_B = 30$ number of atoms. BEC experiences full periodic revivals, however incoming and reflecting BEC wave packets lead to larger matter-wave interference regions at time intervals t = 24–34 and 83–91. Here the color scale represents the density of the BEC.

7. Dynamics of BEC on a hard-wall mirror

Concerning the dynamics of the BEC in a GOST, we consider two cases. First we describe the dynamics of the BEC with $N_B = 1800$ after switching off the evanescent potential and letting the BEC atoms fall on a hard-wall mirror. The latter could be experimentally realized by a blue-detuned far-off-resonant sheet of light, and is modeled theoretically via the boundary condition $V(0) \to \infty$ at $t > 0$. Thus, the BEC of $N_B = 1800$ atoms has the dimensionless mean position $z_0 = 10.7$ and the dimensionless standard deviation $\sigma = 4.28$ at time $t = 0$. We observe the matter-wave interference pattern formed upon releasing the condensate from GOST as shown in figure 10, as atoms impinging on the 'hard-wall' at the origin 'bounce' back. For short times the atoms remain near the hard-wall surface, so the BEC dynamics is characterized by the reflection of atoms from the hard-wall mirror. But for larger times those atoms, which are far away from the hard-wall mirror, are reflected above the hard-wall mirror due to collisions among themselves as shown in figure 10. The number of atoms $N_B = 1800$ is so large that the BEC is staying quite close to the mirror, so we have not seen any total reflection of the BEC wave packet.

In order to see the latter scenario, we need a small number of $N_B = 30$ particles far away from the hard-wall mirror. This is realized by the EW potential $V_0 e^{-(z-20)}$, which could be implemented by trapping atoms in a MOT above the surface, so that, once the EW trap is switched off, the atoms have enough momenta when they hit the hard-wall mirror as shown in figure 11. Similar to experiments of photonic bouncing balls [67] and plasmonic paddle balls [68], the BEC shows significant self-interference patterns, for example in the time intervals t = 24–34 and 83–91 as shown in figure 11, which originate from the interference of incoming and reflecting BEC wave packets. It is worth mentioning that a smaller initial width of the BEC wave packet would lead to finer revivals and a larger initial width of the BEC would lead to larger interference regions. The evolution of a BEC falling under gravity and bouncing off a hard-wall mirror formed by a far-detuned sheet of light was already observed experimentally by Bongs *et al* in both the soft-wall and the hard-wall regime [69]. In the soft-wall regime, they have recorded that the BEC is reflected up to three times off the optical mirror in the lossy environment. Due to a large two-particle coupling strength, which in turn results in a condensate with a larger width, this group also observed a splitting of the BEC into two parts close to the upper turning point of the BEC. This effect is heuristically modeled by a GPE dynamics with assuming that the two-particle interaction strength decreases exponentially in time. In our case we restricted ourselves to the evolution of the BEC with a constant coupling constant, so we did not observe any splitting of the BEC in our simulation, but we do observe the BEC for longer time intervals as shown in figure 11. In our simulation, we observed more than three reflections of the atomic cloud in a lossless environment. The center-of-mass of the BEC wave packet shows periodic revivals with the dimensionless time period $t \approx 58.2$ as shown in figure 11. Quantitatively, the classical revival time can be determined in dimensionless units as $t = 2\sqrt{2z_0/k} = 56.9$, where z_0 represents the mean position of the BEC and the dimensionless energy constant k is defined below equation (3).

8. Conclusion

In summary, we studied the behavior of a Cs BEC in a quasi-1D optical surface trap. We have developed approximate solutions to the GP equation for both small and large numbers of atoms. In the former, we have used the variational ansatz technique, while in the latter we have used the TF approximation. Later on, we compared the analytical approach with numerical results, which agreed quite well for a wide range of atom numbers N_B.

Furthermore, we have numerically reproduced the experimental result of [37], where a 2D BEC is confined in the radial direction, but is allowed to expand in the vertical direction freely. This indicates that our analysis could be extended beyond the 1D case. Our model suggests that for a small particle number N_B the BEC retains its Gaussian shape in the expansion and falls due to gravity. As suggested by figure 9, for larger number of atoms, the standard deviation does not expand as fast as compared to small number of particles, therefore we conclude that the initial number of the particles plays a significant role in the expansion of the BEC cloud. Afterwards, we investigated the dynamics of the BEC in the presence of gravity and a hard-wall boundary condition, where we observed self-interferences and revivals of the wave packet. The observation of the bouncing of the BEC can be used to characterize and determine mirror properties such as roughness and steepness. All our results can be applied to develop atomic interferometers for a BEC.

Acknowledgments

We would like to acknowledge Antun Balaž and Dwight Whitaker for their insightful comments. We also gratefully acknowledge support from the German Academic Exchange Service (DAAD). This work was also supported in part by the German Research Foundation (DFG) via the Collaborative Research Center SFB/TR49 'Condensed Matter Systems with Variable Many-Body Interactions'.

References

[1] Mermin N D and Wagner H 1966 *Phys. Rev. Lett.* **17** 1133–6
[2] Hohenberg P C 1967 *Phys. Rev.* **158** 383–6
[3] Görlitz A *et al* 2001 *Phys. Rev. Lett.* **87** 130402
[4] Schreck F, Khaykovich L, Corwin K L, Ferrari G, Bourdel T, Cubizolles J and Salomon C 2001 *Phys. Rev. Lett.* **87** 080403
[5] Petrov D S, Gangardt D M and Shlyapnikov G V 2004 *J. Phys. IV France* **116** 5–44
[6] Moritz H, Stöferle T, Köhl M and Esslinger T 2003 *Phys. Rev. Lett.* **91** 250402
[7] Hellweg D, Cacciapuoti L, Kottke M, Schulte T, Sengstock K, Ertmer W and Arlt J J 2003 *Phys. Rev. Lett.* **91** 010406
[8] Tolra B L, O'Hara K M, Huckans J H, Phillips W D, Rolston S L and Porto J V 2004 *Phys. Rev. Lett.* **92** 190401
[9] Kinoshita T, Wenger T and Weiss D S 2005 *Phys. Rev. Lett.* **95** 190406
[10] Chuu C S, Schreck F, Meyrath T P, Hanssen J L, Price G N and Raizen M G 2005 *Phys. Rev. Lett.* **95** 260403
[11] Hofferberth S, Lesanovsky I, Fischer B, Schumm T and Schmiedmayer J 2007 *Nature* **449** 324–7
[12] Eckart M, Walser R and Schleich W P 2008 *New J. Phys.* **10** 045024
[13] Pethick C J and Smith H 2008 *Bose–Einstein Condensation in Dilute Gases* 2nd edn (Cambridge: Cambridge University Press)
[14] Olshanii M 1998 *Phys. Rev. Lett.* **81** 938–41
[15] Petrov D S, Shlyapnikov G V and Walraven J T M 2000 *Phys. Rev. Lett.* **85** 3745–9
[16] Bergeman T, Moore M G and Olshanii M 2003 *Phys. Rev. Lett.* **91** 163201
[17] Paredes B, Widera A, Murg V, Mandel O, Folling S, Cirac I, Shlyapnikov G V, Hansch T W and Bloch I 2004 *Nature* **429** 277–81
[18] Kinoshita T, Wenger T and Weiss D S 2004 *Science* **305** 1125–8
[19] Haller E, Gustavsson M, Mark M J, Danzl J G, Hart R, Pupillo G and Nägerl H C 2009 *Science* **325** 1224–7
[20] Stock S, Hadzibabic Z, Battelier B, Cheneau M and Dalibard J 2005 *Phys. Rev. Lett.* **95** 190403
[21] Gillen J I, Bakr W S, Peng A, Unterwaditzer P, Fölling S and Greiner M 2009 *Phys. Rev.* A **80** 021602
[22] Vetsch E, Dawkins S, Mitsch R, Reitz D, Schneeweiss P and Rauschenbeutel A 2012 *IEEE J. Quant. Elect.* **18** 1763–70
[23] Benseghir A, Abdullah W A T W, Baizakov B B and Abdullaev F K 2014 *Phys. Rev.* A **90** 023607
[24] Cook R J and Hill R K 1982 *Opt. Commun.* **43** 258–60
[25] Balykin V and Letokhov V 1987 *Opt. Commun.* **64** 151–6
[26] Liston G, Tan S and Walls D 1995 *Appl. Phys.* B **60** 211–27
[27] Wallis H, Dalibard J and Cohen-Tannoudji C 1992 *Appl. Phys.* B **54** 407–19
[28] Wallis H 1996 *J. Opt. B: Quantum Semiclass. Opt.* **8** 727
[29] Aminoff C G, Steane A M, Bouyer P, Desbiolles P, Dalibard J and Cohen-Tannoudji C 1993 *Phys. Rev. Lett.* **71** 3083–6
[30] Marzlin K P and Audretsch J 1996 *Phys. Rev.* A **53** 4352–9
[31] Saif F, Bialynicki-Birula I, Fortunato M and Schleich W P 1998 *Phys. Rev.* A **58** 4779–83
[32] Akram J and Saif F 2008 *J. Russ. Laser. Res.* **29** 538–43
[33] Nesvizhevsky V V *et al* 2002 *Nature* **415** 297–9
[34] Ovchinnikov Y B, Manek I and Grimm R 1997 *Phys. Rev. Lett.* **79** 2225–8
[35] Hammes M, Rychtarik D, Druzhinina V, Moslener U, Manek-Hönninger I and Grimm R 2000 *J. Mod. Opt.* **47** 2755–67
[36] Domokos P and Ritsch H 2001 *Europhys. Lett.* **54** 306
[37] Rychtarik D, Engeser B, Nägerl H C and Grimm R 2004 *Phys. Rev. Lett.* **92** 173003
[38] Colombe Y, Kadio D, Olshanii M, Mercier B, Lorent V and Perrin H 2003 *J. Opt. B: Quantum Semiclass. Opt.* **5** S155
[39] Colombe Y, Mercier B, Perrin H and Lorent V 2005 *Phys. Rev.* A **72** 061601
[40] Perrin H, Colombe Y, Mercier B, Lorent V and Henkel C 2006 *J. Phys. B: At. Mol. Opt. Phys.* **39** 4649
[41] Gattobigio G L, Couvert A, Georgeot B and Guéry-Odelin D 2010 *New J. Phys.* **12** 085013
[42] Melezhik V S and Schmelcher P 2011 *Phys. Rev.* A **84** 042712
[43] Saeidian S, Melezhik V S and Schmelcher P 2012 *Phys. Rev.* A **86** 062713
[44] Wang Y J, Anderson D Z, Bright V M, Cornell E A, Diot Q, Kishimoto T, Prentiss M, Saravanan R A, Segal S R and Wu S 2005 *Phys. Rev. Lett.* **94** 090405
[45] Jöllenbeck S, Mahnke J, Randoll R, Ertmer W, Arlt J and Klempt C 2011 *Phys. Rev.* A **83** 043406
[46] Petrovic J, Herrera I, Lombardi P, Schäfer F and Cataliotti F S 2013 *New J. Phys.* **15** 043002
[47] Jian B and van Wijngaarden W A 2014 *J. Phys. B: At. Mol. Opt. Phys.* **47** 215301
[48] Kamchatnov A 2004 *J. Exp. Theor. Phys.* **98** 908–17
[49] Carretero-González R, Frantzeskakis D J and Kevrekidis P G 2008 *Nonlinearity* **21** R139
[50] Lennard-Jones J E 1932 *Trans. Faraday Soc.* **28** 333–59
[51] Courtois J Y, Courty J M and Mertz J C 1996 *Phys. Rev.* A **53** 1862–78
[52] Casimir H B G and Polder D 1948 *Phys. Rev.* **73** 360–72
[53] Landragin A, Courtois J Y, Labeyrie G, Vansteenkiste N, Westbrook C I and Aspect A 1996 *Phys. Rev. Lett.* **77** 1464–7
[54] Obrecht J M, Wild R J, Antezza M, Pitaevskii L P, Stringari S and Cornell E A 2007 *Phys. Rev. Lett.* **98** 063201
[55] Robinett R W 2006 *Eur. J. Phys.* **27** 281
[56] Belloni M and Robinett R 2014 *Phys. Rep.* **540** 25–122
[57] Pérez-García V M, Michinel H, Cirac J I, Lewenstein M and Zoller P 1996 *Phys. Rev. Lett.* **77** 5320–3
[58] Pérez-García V M, Michinel H, Cirac J I, Lewenstein M and Zoller P 1997 *Phys. Rev.* A **56** 1424–32
[59] Gerton J M, Strekalov D, Prodan I and Hulet R G 2000 *Nature* **408** 692
[60] Colombe Y, Steinmetz T, Dubois G, Linke F, Hunger D and Reichel J 2007 *Nature* **450** 272–6
[61] Javanainen J and Ruostekoski J 2006 *J. Phys. A: Math. Gen.* **39** L179
[62] Vudragović D, Vidanović I, Balaź A, Muruganandam P and Adhikari S K 2012 *Comput. Phys. Commun.* **183** 2021–5
[63] Kumar R K, Young-S L E, Vudragović D, Balaž A, Muruganandam P and Adhikari S 2015 *Comput. Phys. Commun.* **195** 117–28
[64] Lončar V, Balaž A, Bogojević A, Škrbić S, Muruganandam P and Adhikari S K 2016 *Comput. Phys. Commun.* **200** 406

[65] Satarić B, Slavnić V, Belić A, Balaž A, Muruganandam P and Adhikari S K 2016 *Comput. Phys. Commun.* **200** 411
[66] Yin J 2006 *Phys. Rep.* **430** 1–16
[67] Della Valle G, Savoini M, Ornigotti M, Laporta P, Foglietti V, Finazzi M, Duò L and Longhi S 2009 *Phys. Rev. Lett.* **102** 180402
[68] Liu W, Neshev D N, Miroshnichenko A E, Shadrivov I V and Kivshar Y S 2011 *Phys. Rev.* A **84** 063805
[69] Bongs K, Burger S, Birkl G, Sengstock K, Ertmer W, Rzazewski K, Sanpera A and Lewenstein M 1999 *Phys. Rev. Lett.* **83** 3577–80